

# In Vitro Validation of Clearing Clogged Vessels using Microrobots

Abdelrahman Hosney<sup>\*†</sup>, Joseph Abdalla<sup>\*†</sup>, Ibrahim S. Amin<sup>\*†</sup>, Nabila Hamdi<sup>\*</sup> and Islam S. M. Khalil<sup>\*</sup>

**Abstract**—We achieve mechanical grinding of blood clots using helical microrobots with average diameter of 300  $\mu\text{m}$  inside catheter segments. The helical microrobot is steered and propelled under the influence of rotating magnetic fields (20 mT). These fields are generated using a magnetic-based robotic system with two rotating dipole fields. First, we analyze the optimal configuration of the rotating dipole fields with respect to the helical microrobot to maximize the efficiency of the grinding. This analysis is done using gelatin thrombus model. Not only do we find that an offset (distance between the rotating dipole fields and the dipole of the microrobot) of 15 mm exerts an additional magnetic force to assist the grinding, but we also observe that the drilling time through the thrombus model is decreased by 39%. Second, we prepare blood clots and develop an image processing algorithm to calculate the size of the blood clot during drilling. The drilling decreases the size (disk shaped clots with diameter and length of 3 mm and 5 mm, respectively) of the blood clot by approximately 50% in 36 minutes. The demonstrated *in vitro* grinding experiments using helical microrobots provide broad possibilities in targeted therapy and biomedical applications.

## I. INTRODUCTION

Atherothrombosis is a leading cause of mortality on a worldwide scale [1]. A serious manifestation of atherothrombosis is the ST-segment elevation myocardial infarction (STEMI), in which clinical trials demonstrate that coronary recanalization must be early and rapid with complete reflow [2]. STEMI is currently treated by emergency Primary Percutaneous Coronary Intervention (PPCI). However, the mortality rate increases in case of long delays ( $>90$  minutes) or lack of significant infrastructure and experienced operators [3], [4]. A common alternative to PPCI is intravenous (IV) thrombolytic therapy. However, this alternative has potential fatal hemorrhagic complications [5]. The mentioned problems can be partially overcome by using microrobotic systems [6], [7]. The human circulatory system might allow untethered magnetically-actuated helical microrobots [8], [9], [10], [11] to reach deep-seated regions of the body by vessels [12]. The controlled motion of these microrobots in fluidic environment would enable us to achieve non-trivial *in vivo* tasks such as clearing blood clots, targeted drug delivery, and removing atherosclerotic plaques. Very recently, Servant *et al.* have achieved magnetically controlled navigation of a swarm of artificial bacterial flagella in the

This work was supported by funds from the German University in Cairo and the DAAD-BMBF funding project. The authors also acknowledge the funding from the Science and Technology Development Fund in Egypt (No. 23016).

<sup>\*</sup>The authors are affiliated with the German University in Cairo, New Cairo City 11835, Egypt.

<sup>†</sup>The authors assert equal contribution and joint first authorship.

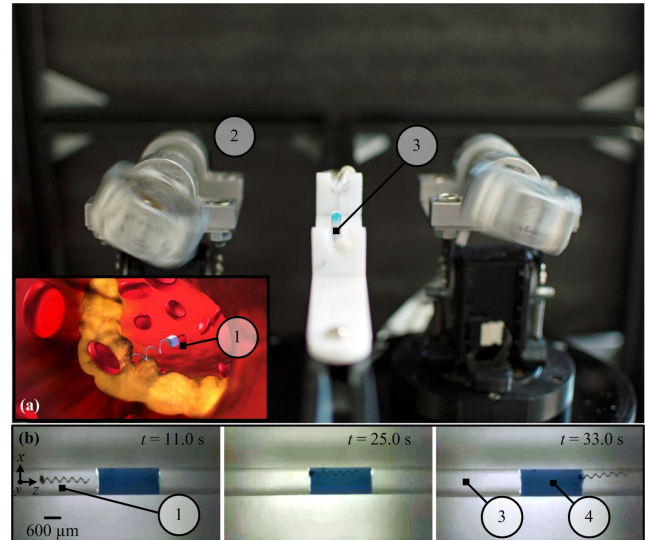


Fig. 1. Grinding of blood clots is achieved using a helical microrobot ① and a magnetic-based robotic system ② with two rotating dipole fields. The helical microrobot is steered and propelled under the influence of the rotating magnetic fields that are generated using the two rotating dipole fields inside catheter segment ③. (a) A schematic representation of clearing a clogged blood vessel using a microrobot. This schematic representation is designed using Blender (Blender 2.71, Blender Foundation, Entrepotdok, Amsterdam, The Netherlands). (b) Penetration of a gelatin (blue-dyed 5% w/w gelatin) thrombus model ④ is achieved in 33 seconds. The average swimming speed of the helical microrobot is 110  $\mu\text{m}/\text{s}$  at rotating magnetic field of 6 Hz.

peritoneal cavity of a mouse *in vivo*. It has been previously demonstrated that these microrobots can be controlled under the influence of the rotating magnetic fields that are generated using electromagnetic systems with closed- and open-configurations [14], [15]. Peyer *et al.* [16] and Tottori *et al.* [17] have demonstrated that helical microrobots enable propulsion through tissue and bodily fluids using low-strength rotating magnetic fields. In addition, Schamel *et al.* have demonstrated that helical nano-propellers can be controllably steered through biological tissue. This propulsion has been achieved using triaxial Helmholtz coil system that limits the workspace to the common center of the coils [18]. In addition, it is difficult to scale the triaxial Helmholtz coil system up to the size of *in vivo* devices [7]. It is also difficult to incorporate a clinical imaging modality to electromagnetic systems with closed-configurations during *in vivo* trials [20]. Fountain *et al.* [15] and Mahoney *et al.* [21] have overcome these challenges by using non-uniform fields generated using single rotating permanent magnet. Nelson *et al.* [22] have utilized the non-uniformity of the rotating field in generating

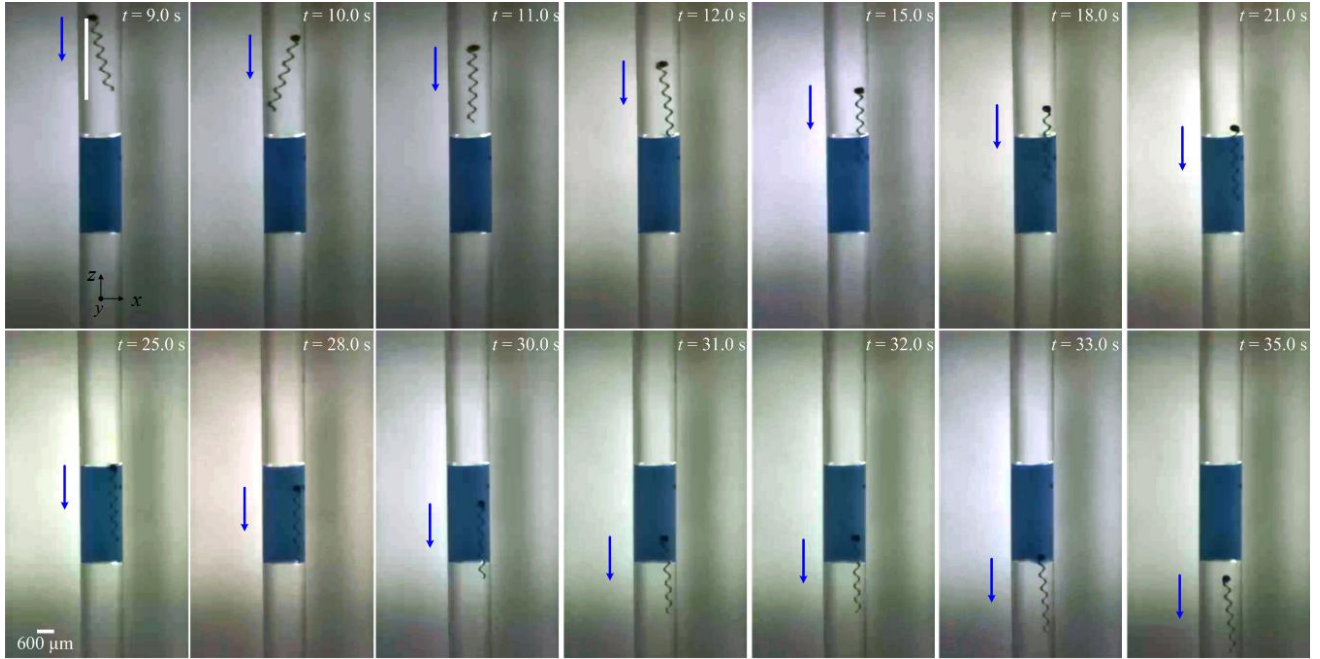


Fig. 2. Penetration of gelatin using a helical microrobot with diameter of  $300\text{ }\mu\text{m}$ . The gelatin (blue-dyed 5% w/w gelatin) is prepared and inserted inside a catheter segment. At time,  $t=9$  seconds, rotating magnetic fields are applied using the two rotating dipole fields, and penetration of the gelatin starts at time,  $t=12$  seconds. The helical microrobot drills through the gelatin and exits at time,  $t=33$  seconds. The average speed of the microrobot is calculated to be  $408\text{ }\mu\text{m/s}$  in the silicone oil and  $357\text{ }\mu\text{m/s}$  in the gelatin. The blue arrow indicates the direction of motion of the helical microrobot. Please refer to the accompanying video that demonstrates the penetration of gelatin using a helical microrobot.

two independent rotating magnetic fields using a single magnet dipole. It has also been shown that the utilization of two synchronized rotating dipole fields mitigates the lateral oscillation of the helical microrobot [23], and allows propulsion in three-dimensional (3D) space with gravity compensation [24], [25]. Mahoney *et al.* [27] have experimentally demonstrated the existence of magnetic torques that can simultaneously stabilize and destabilize a helical microrobot in soft-tissue. An empirical model of helical microrobot has been developed from experimental measurements in an agar gel phantom to predict the effect of the tissue material and the role of the microrobot geometry on the resulting trajectory [28]. Despite this progress in fabrication, actuation, and control of helical microrobots, numerous challenges remain for translating these microrobots into *in vivo* applications.

In this work, we achieve mechanical grinding of blood clots using helical microrobots inside catheter segments. First, we use gelatin thrombus model to optimize the drilling parameters (magnetic field rotation speed and offset between the microrobot and dipole fields) of the helical microrobot using a magnetic-based robotic system (Fig. 1) with two rotating dipole fields [25]. This system can be scaled up to the size of *in vivo* applications. Second, we drill through blood clots and study the relation between the drilling time and the size of the clot. This size is calculated using a morphological filtering algorithm. The remainder of this paper is organized as follows: Section II provides descriptions pertaining to the propulsion using two synchronized rotating dipole fields, preparation of gelatin thrombus model, and analysis of the

optimal configuration of the helical microrobot with respect to the rotating dipole fields. Grinding of blood clots experiments and analysis of the relation between the drilling time and the size of the blood clots are included in Section III. Finally, Section IV concludes and provides directions for future work.

## II. DRILLING OF GELATIN THROMBUS MODEL

Propulsion of the helical microrobots is achieved inside catheter segments that contain silicone oil and gelatin using a magnetic system with rotating dipole fields.

### A. Magnetic System with Two Rotating Dipole Fields

Locomotion of the microrobot is achieved by the helical propulsion using rotating dipole fields. The external magnetic field exerts a magnetic torque to rotate the microrobot, and generates a propulsive force. We observe that this force allows the microrobot to swim in a fluid and overcome drag force, as shown in Fig. 2. However, drilling through blood clots requires greater propulsive force than that required for swimming. The magnetic field gradients along  $y$ - and  $z$ -axis almost vanish at the position of the microrobot, whereas field gradient along  $z$ -axis exists for a non-zero offset between the rotating dipole fields and the microrobot. The magnetic field components are measured at different offset distances using a calibrated 3-axis digital Teslameter (Senis AG, 3MH3A-0.1%-200mT, Neuhoefstrasse, Switzerland). The magnitude of the magnetic field is calculated and the magnetic field gradient along  $z$ -axis is numerically determined, as shown in Fig. 3. Maximum magnetic torque is exerted on the magnetic

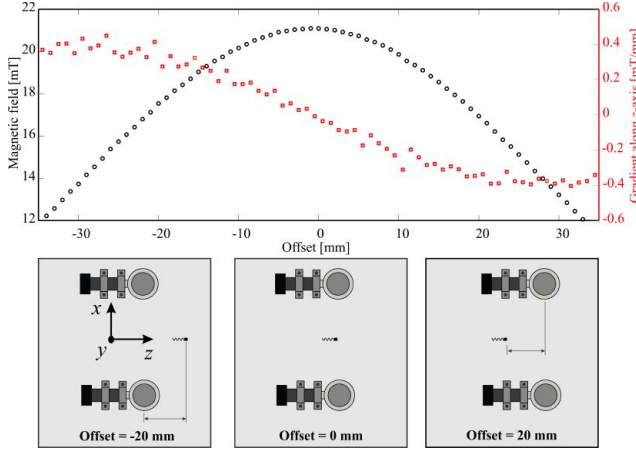


Fig. 3. Magnetic field and field gradient along  $z$ -axis versus the offset between the dipole fields and the helical microrobot. An offset of  $\pm 15$  mm allows the microrobot to combine the propulsive and magnetic forces to decrease the drilling time of the blood clots, whereas zero offset provides pure magnetic torque on the microrobot. The magnetic field is measured using a calibrated 3-axis digital Teslameter (Senis AG, 3MH3A-0.1%-200mT, Neuhoefstrasse, Switzerland), and the field gradient is calculated numerically using MATLAB R2014a (MathWorks, Natick, Massachusetts, U.S.A).

dipole moment of the helical microrobot for zero offset. At this configuration, the motion of the helical microrobot is only due to its helical propulsion since the magnetic field gradient is almost zero. Non-zero offset between the helical microrobot and the dipole field provides an additional pulling magnetic force and a decrease in the exerted magnetic torque. Therefore, we devise an offset of 15 mm between the rotating dipole fields and the helical microrobot during the drilling of the blood clots. Preliminary drilling trials are done using gelatin thrombus model with range of offset distances from 0 mm to 40 mm to study the effect of the offset on the drilling time.

#### B. Penetration of Gelatin Thrombus Model

A thrombus model is prepared using 5% w/w gelatin (El Nasr Pharmaceutical Chemicals Co., El Obour City, Egypt) and blue-dyed distilled water. First, distilled water is dyed and heated to 60°C then the gelatin is added under continuous stirring to obtain a clear mixture. The PVC tube of an IV infusion set (Ultramedumic, Cairo, Egypt) of 3 mm in inner-diameter is cut into 20 cm segments to mimic a human blood vessel. A volume of 65  $\mu$ l of liquid gelatin is inserted into each catheter segment. The samples are refrigerated at 4°C for 18 hours prior to the *in vitro* trials. The catheters are filled with silicone oil (Wacker Chemie AG, Burghausen, Germany) with viscosity of 1 Pa.s before drilling. Silicone oil is a hydrophobic medium, which is immiscible with gelatin preventing dissolving the gelatin of the thrombus model.

A representative experimental result of drilling through the thrombus model is provided in Fig. 2. The helical microrobot is propelled in the silicone oil using a rotating dipole field of 6 Hz. The microrobot swims towards the thrombus model at an average speed of 408  $\mu$ m/s and contact is observed at time,  $t=12$  seconds. The microrobot drills through the

TABLE I  
PSEUDO-CODE OF THE MORPHOLOGICAL FILTERING ALGORITHM THAT IS USED TO CALCULATE THE SIZE OF THE BLOOD CLOT.

**Inputs:** Drilling video of blood clot (vid), number of frames ( $f$ ), image (img) width in pixels ( $x$ ), image length in pixels ( $y$ ), contrast threshold (thr).

**Output:** Size of the blood clot as a percentage of its initial size (initsize) against the duration of the video.

```

 $t = 1$ 
while  $t < f$  do
    size, $i,j \leftarrow 0$ ;
    img  $\leftarrow$  read(vid,  $t$ );
    img  $\leftarrow$  grayscale(img);
    img  $\leftarrow$  binary(img,thr);
    img  $\leftarrow$  opening reconstruction(img);
    while  $i < x$  do
        while  $j < y$  do
            if img( $i,j$ ) == 1
                size  $\leftarrow$  size + 1;
                 $j \leftarrow j+1$ ;
            end
             $i \leftarrow i+1$ ;
        end
        if  $t == 1$ 
            initsize = size;
            size = 100;
        else
            size  $\leftarrow$  100  $\left(\frac{\text{size}}{\text{initsize}}\right)$ ;
        plot ( $t$ ,size);
         $t \leftarrow t + 1$ ;
    end

```

thrombus model at an average speed of 357  $\mu$ m/s, and exits from the gelatin at time,  $t=33$  seconds. This trial is done at an offset of 10 mm between the rotating dipole fields and the helical microrobot (Fig. 3). The drilling time is calculated to be approximately 20 seconds. Please refer to the accompanying video that demonstrates drilling through thrombus model using a helical microrobot.

We repeat this experiment at a range of offset distances, as shown in Fig. 4. The drilling time of the thrombus model decreases for a configuration of non-zero offset. The drilling time reaches to an asymptote of approximately 18 seconds for non-zero offset between the rotating dipole fields and the microrobot. The average drilling time is calculated from 5 trials at each offset using the same helical microrobot. Therefore, we adjust the offset between the microrobot and the dipole field to be 15 mm throughout our experimental work to decrease the drilling time through the blood clots.

### III. GRINDING OF THE BLOOD CLOTS

Blood clots are prepared and inserted into catheter segments. The size of the blood clots is monitored using morphological filtering throughout the drilling operation.

#### A. Preparation of the Blood Clots

Venous blood is drawn from three male donors (the first authors, average age is 23 years) into a vacutainer without anticoagulant. Local Institutional Ethical Board approval is obtained for the preparation protocol of the blood clots, and

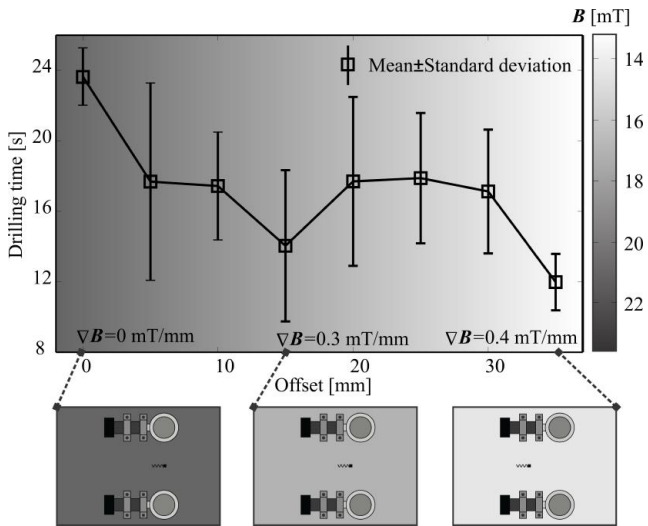


Fig. 4. Drilling time is calculated versus a range of offset distances between the helical microrobot and the dipole fields. The average drilling time is calculated using 5 trials at each offset. Gelatin thrombus model is used in this experiment and the helical microrobot is propelled at frequency of 6 Hz. Drilling is achieved using pure magnetic torque at zero offset, whereas a combination of magnetic torque and a pulling magnetic force achieve faster drilling for non-zero offset.

donors gave written informed consent. Blood clots are prepared based on the protocol proposed by Hoffmann *et al.* [26] with the following modifications:

- 1) The vacutainer is incubated in controlled temperature water bath (Gesellschaft für Labortechnik, Germany) at 37°C for 1 hour. The blood coagulates to form a mother clot (Fig. 5(a)) with a long columnar shape;
- 2) The mother clot is laid on a plastic sheet and rolled for a distance of 50 cm to dry from adherent serum, and left for 5 minutes to air dry and then finally roll dried again for a further 50 cm;
- 3) The mother clot is cut into daughter clots of 3 mm in length. Each daughter clot (Fig. 5(b)) is roll dried for 30 cm four times with air drying for 1 minute after each time;
- 4) Catheter segments are cut (as previously described) and each daughter clot is loaded into a catheter segment;
- 5) The catheter segment is filled proximally and distally with Phosphate Buffered Saline (Lonza BioWhittaker, BE17-516F, Verviers, Belgium), using a 3 mL syringe (Sung Shim Medical Co., Ltd., Korea) and its ends are sealed.

The catheter segment is mounted in the center of the two rotating dipole fields and the permanent magnets are moved 15 mm along  $z$ -axis (with respect to the helical microrobot) to optimize the drilling efficiency based on Fig. 3.

### B. Grinding of Blood Clots

Drilling of the blood clot is achieved and the size of the blood clot is calculated. Fig. 6 shows a representative grinding of a blood clot with diameter and width of 3 mm and 5 mm, respectively. The percentage of size reduction

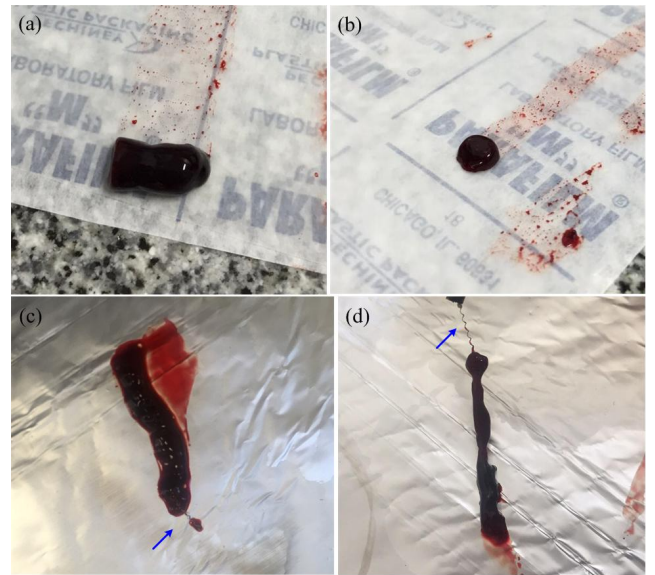


Fig. 5. Pre- and Post-conditions of the blood clots following 20 minutes of drilling using a helical microrobot (blue arrow). (a) The mother clot with a long columnar shape is prepared to provide daughter clots. (b) Daughter clot is cut with length of 3 mm. (c) and (d) Dissolved blood clots after drilling using the microrobot for approximately 20 minutes.

of the blood clot is calculated during the drilling using a real-time image processing algorithm. First, the contrast of the blood clot is increased with respect to the rest of the image. The intensity values in the input image is set to new values such that 1% of the data is saturated at low and high intensities. Second, the images are converted to binary and a threshold is set to allow the darkest features to appear. Third, morphological filtering (erosion, dilation, and reconstruction) is implemented using a diamond-shaped structuring element. A pseudo-code of the morphological filtering is provided in Table I.

A representative drilling through a blood clot is provided in Fig. 6. The rotating magnetic fields are applied at frequency of 6 Hz and the magnetic field at the position of the microrobot is measured to be 20 mT. At time,  $t=244$  seconds, the helical microrobot drills through the blood clot and mixing of blood constituents with the liquid medium is observed throughout the catheter segment. After,  $t=436$  seconds, the blood clot is rotated by the rotation of the microrobot. The rotation of the blood clot results in fluctuation in the calculated size of the blood clot, as shown in Fig. 7. The blood clot takes irregular shapes after a few seconds of drilling. Therefore, the calculated size of the clot varies during rotation. Nevertheless, the calculated size of the clot indicates that a linear decrease (Fig. 7) is achieved with the drilling time. In this representative experiment, the size of the blood clot is decreased by 50% after approximately 36 minutes. All experiments are repeated 10 times, and we observe consistent results. Fig. 8 provides representative pre- and post-conditions of the blood clots subjected to drilling for 20 minutes, at frequency of 6 Hz.

The drilling effect on the blood clot is also assessed by

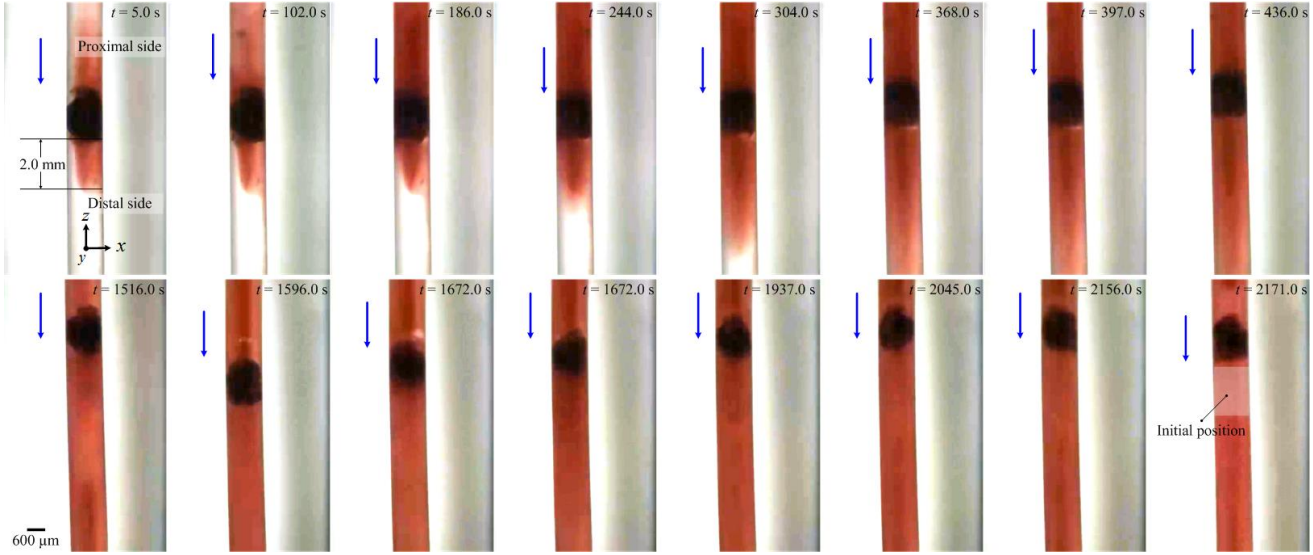


Fig. 6. Grinding of a blood clot with diameter and width of 3 mm and 5 mm, respectively, is achieved using a helical microrobot. The microrobot swims in the phosphate buffered saline at an average speed of 600  $\mu\text{m}/\text{s}$  and contact with the blood clot is observed at time,  $t=5$  seconds. At time,  $t=436$  seconds, the blood clot becomes mobile and both rotation and translation along the catheter segment are observed. In this representative experiment, the size of the blood clot is decreased by 50% following 36 minutes of drilling using the microrobot. Please refer to the accompanying video that demonstrates the grinding of a blood clot using a helical microrobot.

measuring the extent of mixing of blood constituents with the liquid medium lengthwise before and after drilling. The lengthwise mixing of the blood constituents with the liquid medium before drilling is 0.5 cm at the proximal side of the catheter (microrobot is inserted from the proximal side) and 0.44 cm at the distal side. After drilling for 2171 seconds, the mixing of the blood constituents is 7 cm proximally and 6.5 cm distally and also the blood clot moves 0.5 cm from its original position towards the proximal end. Therefore, the relative mixing of the blood constituents is 6.5 cm proximally and 6.0 cm distally. Figs. 5(c) and (d) show the pre- and post-condition of a blood clot following 20 minutes of drilling, respectively. We observe that the size of the blood clot decreases after drilling. Under the current experimental conditions, we do observe that pieces of the blood clot could be broken from the main clot, which might cause a secondary clot in another area of the body. This could be overcome by adding a chemical thrombolytic adjunct to increase the clot dissolution [26].

#### IV. CONCLUSIONS AND FUTURE WORK

We experimentally show that helical microrobot can be used as an efficient tool in drilling blood clots under the influence of rotating dipole fields. The size of the blood clot is decreased by approximately 50% following 36 minutes of drilling using rotating magnetic fields of 20 mT at frequency of 6 Hz. The drilling time of the blood clots is decreased by combining the propulsive and magnetic forces that are generated by the helical rotation and exerted on the magnetic dipole of the microrobot, respectively. An offset of 15 mm between the helical microrobot and the rotating dipole fields allows us to combine the propulsive force and the magnetic force in drilling through the blood clots.

As part of future studies, the mechanical grinding of blood clots will be improved chemically by adding a thrombolytic agent, e.g., streptokinase, to the medium to decrease the drilling time. The mechanical grinding will be compared to the combination of mechanical grinding and chemical lysis. We will study the influence of using multiple helical microrobots to drill simultaneously through the blood clots and decrease the clearing time. In addition, our magnetic system will be adapted by incorporating an ultrasound system to provide the position of the helical microrobot and the size of the blood clots. Drilling of the blood clots will also be done in the presence of simulated body fluid with time-varying flow rates to study the effect of flow on the drilling using helical microrobots.

#### V. ACKNOWLEDGMENTS

The authors would like to thank Ms. Mariam Soliman for assistance with the development of the animation in Fig. 1 and the accompanying video.

#### REFERENCES

- [1] D. Lloyd-Jones *et al.*, “Heart disease and stroke statistics—2010 update: a report from the american heart association”, *Circulation*, vol. 121, no. 7, pp. 46–215, February 2010.
- [2] A. M. Lincoff and E. J. Topol, “Illusion of reperfusion. does anyone achieve optimal reperfusion during acute myocardial infarction?”, *Erratum*, vol. 88, no. 3, pp. 1361–1374, September 1993.
- [3] D. J. Magid, B. N. Calonge, J. S. Rumsfeld, J. G. Canto, P. D. Frederick, N. R. Every, and H. V. Barron , “Relation between hospital primary angioplasty volume and mortality for patients with acute MI treated with primary angioplasty vs thrombolytic therapy”, *The Journal of the American Medical Association*, vol. 284, no. 24, pp. 3131–3138, December 2000.
- [4] J. G. Canto *et al.*, “The volume of primary angioplasty procedures and survival after acute myocardial infarction”, *The New England Journal of Medicine*, vol. 342, no. 21, pp. 1573–1580, May 2000.

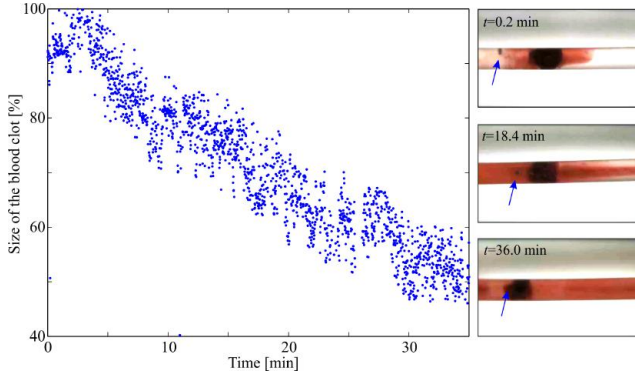


Fig. 7. A representative experimental result of drilling through a blood clot using a helical microrobot. The size of the blood clot is calculated using morphological filtering (erosion, dilation, and reconstruction). The size of the blood clot is decreased by approximately 50% after 36 minutes of drilling, at rotating magnetic field of 6 Hz. The fluctuation of the calculated size is due to the rotation of the blood clot inside the catheter segment. The blood clot takes irregular shapes after drilling and the rotation results in fluctuations at every time instant. Please refer to the accompanying video that demonstrates the experimental drilling through the blood clot.

- [5] The GUSTO Investigators, “An interventional randomized trial comparing four thrombolytic strategies for acute myocardial infarction”, *The New England Journal of Medicine*, vol. 329, no. 10, pp. 673-682, September 1993.
- [6] J. L. F. Gabayno, D. Liu, M. Chang, and Y. Linc, “Controlled manipulation of  $\text{Fe}_3\text{O}_4$  nanoparticles in an oscillating magnetic field for fast ablation of microchannel occlusions”, *Nanoscale*, vol. 7, no. 9, pp. 3947-3953, January 2015.
- [7] B. J. Nelson, I. K. Kaliakatos, and J. J. Abbott, “Microrobots for minimally invasive medicine,” *Annual Review of Biomedical Engineering*, vol. 12, pp. 55-85, April 2010.
- [8] K. E. Peyer, L. Zhang, and B. J. Nelson, “Bio-inspired magnetic swimming microrobots for biomedical applications”, *Nanoscale*, vol. 5, no. 4, pp. 1259-1272, November 2012.
- [9] D. J. Bell, S. Leutenegger, K. M. Hammar, L. X. Dong, and B. J. Nelson, “Flagella-like propulsion for microrobots using a magnetic nanocoil and a rotating electromagnetic field”, in *Proceedings of the IEEE International Conference on Robotics and Automation (ICRA)*, pp. 1128-1133, April 2007.
- [10] J. J. Abbott, K. E. Peyer, L. Dong, and B. Nelson, “How should microrobots swim?” *The International Journal of Robotics Research*, vol. 28, no. 11-12, pp. 1434-1447, July 2009.
- [11] E. M. Purcell, “Life at low reynolds number,” *American Journal of Physics*, vol. 45, no. 1, pp. 3-11, June 1977.
- [12] J. Wang and W. Gao, “Nano/Microscale motors: biomedical opportunities and challenges” *ACS Nano*, vol. 6, no. 7, pp. 5745-5751, July 2012.
- [13] A. Servant, F. Qiu, M. Mazza, K. Kostarelos, and B. J. Nelson, “Controlled in vivo swimming of a swarm of bacteria-like microrobotic flagella”, *Advanced Materials*, vol. 27, no. 19, pp. 2981-2988, April 2015.
- [14] M. P. Kummer, J. J. Abbott, B. E. Kartochvil, R. Borer, A. Sengul, and B. J. Nelson, “OctoMag: an electromagnetic system for 5-DOF wireless micromanipulation,” *IEEE Transactions on Robotics*, vol. 26, no. 6, pp. 1006-1017, December 2010.
- [15] T. W. R. Fountain, P. V. Kailat, and J. J. Abbott, “Wireless control of magnetic helical microrobots using a rotating-permanent-magnet manipulator,” in *Proceedings of the IEEE International Conference on Robotics and Automation (ICRA)*, pp. 576-581, Alaska, USA, May 2010.
- [16] K. E. Peyer, S. Tottori, F. Qiu, L. Zhang, and B. J. Nelson, “Magnetic Helical Micromachines”, *Chemistry*, vol. 19, no. 1, pp. 28-38, January 2013.
- [17] S. Tottori, L. Zhang, F. Qiu, K. K. Krawczyk, and A. Franco-Obregón, and B. J. Nelson, “Magnetic helical micromachines: fabrication, controlled swimming, and cargo transport”, *Advanced Materials*, vol. 24, no. 6, pp. 811-816, February 2012.

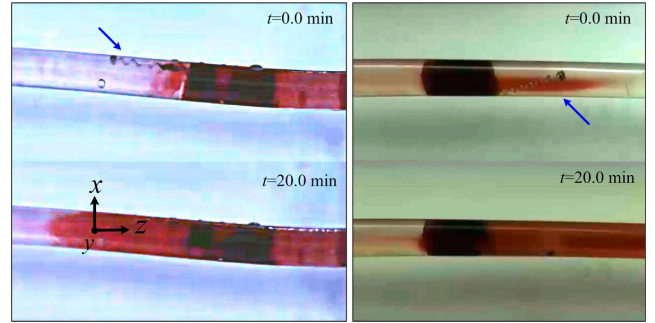


Fig. 8. Representative pre- and post-drilling experimental results of blood clots using helical microrobots (blue arrows). The microrobot is propelled using rotating magnetic field of 20 mT at frequency of 6 Hz, for 20 minutes. Mixing of the blood constituents with the liquid medium is observed after a few seconds of drilling using the microrobot. Left: A helical microrobot rotates counter clockwise and drills through the clot along  $z$ -axis. Right: A helical microrobot drills along negative  $z$ -axis. Please refer to the accompanying video that demonstrates the pre- and post-conditions of the blood clots.

- [18] K. E. Peyer, A. W. Mahoney, L. Zhang, J. J. Abbott, and B. J. Nelson, “*Microbiorobotics*”, Springer-Verlag Berlin Heidelberg, March 2012.
- [19] D. Schamel, A. G. Mark, J. G. Gibbs, C. Miksch, K. I. Morozov, A. M. Leshansky, P. Fischer, “Nano-Propellers and their actuation in complex viscoelastic media”, *ACS Nano*, vol. 8, no. 9, pp. 8794-8801, June 2014.
- [20] I. S. M. Khalil, P. Ferreira, R. Eleutério, C. L. de Korte, and S. Misra, “Magnetic-Based closed-loop control of paramagnetic microparticles using ultrasound feedback,” in *Proceedings of the IEEE International Conference on Robotics and Automation (ICRA)*, pp. 3807-3812, Hong Kong, China, June 2014.
- [21] A. W. Mahoney, D. L. Cowan, K. M. Miller, and J. J. Abbott, “Control of untethered magnetically actuated tools using a rotating permanent magnet in any position,” in *Proceedings of the IEEE International Conference on Robotics and Automation (ICRA)*, pp. 3375-3380, Minnesota, USA, May 2012.
- [22] N. D. Nelson and J. J. Abbott, “Generating two independent rotating magnetic fields with a single magnetic dipole for the propulsion of untethered magnetic devices,” in *Proceedings of the IEEE International Conference on Robotics and Automation (ICRA)*, pp. 4056-4061, Seattle, Washington, USA, May 2005.
- [23] M. E. Alshafeei, A. Hosney, A. Klingner, S. Misra, and I. S. M. Khalil, “Magnetic-Based motion control of a helical robot using two synchronized rotating dipole fields,” in *Proceedings of the IEEE RAS/EMBS International Conference on Biomedical Robotics and Biomechatronics (BioRob)*, pp. 151-156, São Paulo, Brazil, August 2014.
- [24] A. W. Mahoney and J. J. Abbott, “Managing magnetic force applied to a magnetic device by a rotating dipole field,” *Applied Physics Letters*, 99, September 2011.
- [25] A. Hosney, A. Klingner, S. Misra, and I. S. M. Khalil, “Propulsion and steering of helical magnetic microrobots using two synchronized rotating dipole fields in three-dimensional space,” in *Proceedings of the IEEE/RSJ International Conference of Robotics and Systems (IROS)*, pp. 1988-1993, Hamburg, Germany, November 2015.
- [26] A. Hoffmann and H. Gill, “Diastolic timed vibro-percussion at 50Hz delivered across a chest wall sized meat barrier enhances clot dissolution and remotely administered streptokinase effectiveness in an in-vitro model of acute coronary thrombosis”, *Thrombosis Journal*, vol. 10, no. 23, pp. 1-16, November 2012.
- [27] A. W. Mahoney, N. D. Nelson, E. M. Parsons, and J. J. Abbott “Non-ideal behaviors of magnetically driven screws in soft tissue”, in *Proceedings of the IEEE International Conference of Robotics and Systems (IROS)*, pp. 3559-3564, Vilamoura, Algarve, October 2012.
- [28] N. D. Nelson, J. Delacenserie, and J. J. Abbott “An empirical study of the role of magnetic, geometric, and tissue properties on the turning radius of magnetically driven screws”, in *Proceedings of the IEEE International Conference on Robotics and Automation (ICRA)*, pp. 5372-5377, Karlsruhe, Germany, May 2013.